

# Chord bearing capacity in long-span tubular trusses

B. Kozy<sup>†</sup>, R. Boyle<sup>‡</sup> and C. J. Earls<sup>‡†</sup>

*Department of Civil & Environmental Engineering, University of Pittsburgh, Pittsburgh,  
Pennsylvania, 15261, USA*

*(Received November 2, 2004, Accepted September 15, 2005)*

**Abstract.** The capacity of tubular truss chords subjected to concentrated reaction forces in the vicinity of the open end (i.e., the bearing region) is not directly treated by existing design specifications; although capacity equations are promulgated for related tubular joint configurations. The lack of direct treatment of bearing capacity in existing design specifications seems to represent an unsatisfactory situation given the fact that connections very often control the design of long-span tubular structures comprised of members with slender cross-sections. The case of the simple-span overhead highway sign truss is studied, in which the bearing reaction is applied near the chord end. The present research is aimed at assessing the validity of adapting existing specifications' capacity equations from related cases so as to be applicable in determining design capacity in tubular truss bearing regions. These modified capacity equations are subsequently used in comparisons with full-scale experimental results obtained from testing carried out at the University of Pittsburgh.

**Keywords:** side wall bearing; tubular member bearing; long-span trusses; bearing limit state; nonlinear finite element analysis; circular HSS.

---

## 1. Introduction

Circular Hollow Structural Shapes (HSS) possess a very efficient cross-section for the resistance of compressive and torsional stresses as a result of their closed, symmetrical geometry. A given circular HSS member has both a smaller surface area and greater torsional rigidity relative to a comparable open section member of the same weight. Although the material cost is higher for the grades of steel typically specified for hollow sections, this increased cost is typically offset by the lower construction weight deriving from greater structural efficiency, the smaller coating area required for corrosion protection (paint or galvanizing) due to the enclosed nature of the section, and the reduction in fabrication cost by the application of simple joints without stiffening elements. Combine this with the pleasing aesthetics of the HSS, and one can see why tubular members are quickly gaining popularity in structural applications. In particular, the circular HSS has become the member of choice in applications that involve wind, water, or wave loading due to its low drag coefficient. Common structures that utilize the circular HSS include offshore platforms, space trusses in buildings and stadiums, and overhead highway sign structures (see Fig. 1). It is one design aspect of the last of these applications that has motivated the current research. However, the findings will be of interest to researchers and

---

<sup>†</sup>Adjunct Lecturer

<sup>‡</sup>Graduate Research Assistant

<sup>‡†</sup>Associate Professor & William Kepler Whiteford Faculty Fellow, Corresponding author, E-mail: [earls@enr.pitt.edu](mailto:earls@enr.pitt.edu)



Fig. 1 Tri-chord overhead highway sign structure

engineers working with many types of tubular structures.

One of the primary challenges in designing a safe, cost-effective tubular structure is in the detailing of the connections. Connections in tubular structures can be simple HSS-to-HSS connections, connections between an open section and an HSS, or connections made through gusset plates. The last two of these are sometimes referred to as “plate-type” connections. In the specialized case of a truss, the connections usually consist of one or more smaller branch members that are attached to a continuous chord that passes through the connection work point. These joints can be classified as a T-Connection, Y-Connection, Cross-Connection, or a K-Connection depending on the geometry. For design, special attention must be given to ensure that the connection does not fail by way of punching shear rupture, chord wall plastification, general collapse, or by some other local failure mechanism. The behavior of HSS-to-HSS connections has been researched and is well understood, but less work has been done in the area of plate-type HSS connections.

In the design of tubular structures such as overhead highway sign trusses, the desire is to have chord members with a large radius of gyration (larger diameter with thinner walls) so as to increase axial compressive resistance while at the same time reducing member weight. However, such an approach as this usually leads to a trade-off since joint capacities are typically reduced due to the decreased capacity in thin chord walls. Therefore as a compromise, it is recommended that chord members be sized with relatively thick walls and branch members be sized with relatively thin walls (AISC 2000). If the joint design demands that the chord wall be excessively thick, the designer should then consider reinforcing the joint with stiffeners or grouting rather than using a greater chord thickness, in the interest of economy. Unfortunately, it is not always a simple matter to determine under what circumstances chord wall demands become excessive.

The focus of the current work is a portion of long-span tubular trusses that is not addressed directly in the research literature or existing design specifications: the bearing region. For simple-span trusses, the primary load path for the reaction force developed at the support is from the bearing, through the chord, and directly into the first intermediate vertical member. Therefore, the overall bearing capacity is influenced by all of these member proportions and their spacing with respect to one another.

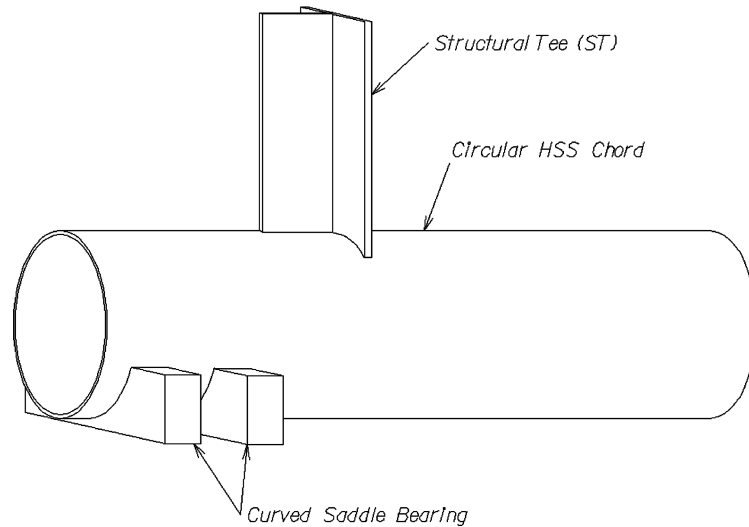


Fig. 2 Bearing configuration under investigation

Based on current US design practice in overhead highway sign trusses, a bearing connection detail involving curved steel saddle bearings and a Structural Tee (ST) intermediate member connected directly to a large-diameter circular HSS chord, near its open end, is considered (see Fig. 2). While some research has been done on concentrated loads applied to HSS walls through gusset plates and HSS branch members, very little work has been done on loads applied directly through the end of open sections; and no previous work has been found in the literature concerning the cases of saddle-type bearings located at chord ends or an ST bearing on a circular HSS chord.

## 2. Review of existing specifications

The governing specification for the design of highway overhead sign structures in the US is the *Standard Specifications for Structural Supports for Highway Signs, Luminaires and Traffic Signals, 4<sup>th</sup> Edition* (AASHTO 2001). Currently, this specification does not address the capacity of tubular connections at all; a potentially serious omission since joint related limit states often control the overall structural capacity (Li and Earls 2002). The design engineer must look beyond this omission and recognize the need for checking joint strengths by consulting other specifications for guidance. American specifications that do address connection capacities in tubular structures are the *Load and Resistance Factor Design Specification for Steel Hollow Structural Sections* (AISC 2000), which can be found in Part 16 of *AISC LRFD Manual 3<sup>rd</sup> Edition* (AISC 2001), and AWS D1.1 (AWS 2004). Also, more detailed guidance and examples are provided in the *AISC Hollow Structural Sections Connection Manual* (AISC 1997a).

The *AISC Hollow Structural Sections Connections Manual* (AISC 1997a) is the definitive American design manual representing the state-of-the-art in hollow structural section connection design and detailing. This manual treats specific design topics related to: dimensions and properties of HSS members; welding practice; issues related to bolting; simple shear connections; moment connections;

tension and compression connections; cap plates, base plate, and column splices; and welded truss connections. In addition, the manual contains the *Specification for the Design of Steel Hollow Structural Sections* (AISC 1997b), which deals specifically with HSS design issues related to: material properties; loads and load combinations; effective net area for tension members; local plate buckling; limiting slenderness ratios; and design for tension, compression, flexure, shear, torsion, combined loading, and the localized effects of various type of transverse loading scenarios; weld design; truss connection design; and fabrication requirements.

The *AISC Hollow Structural Sections Connections Manual* (AISC 1997a) has a Canadian counterpart in the *CISC Hollow Structural Section Connections and Trusses Design Guide* (Packer 1997). This Canadian Manual treats many of the same topics of its American counterpart as well as several additional topics such as: material property and cross-sectional geometric definitions; standard truss design; standard truss welded connections; non-standard truss design; multiplanar welded connections; HSS-to-HSS moment connections; bolted HSS connections; fabrication, welding, and inspection; beam to HSS column connections; trusses and base plates to HSS connections; plate to HSS connections; HSS welded connections subjected to fatigue loading; and standard truss examples.

While it may appear from the forgoing that the Canadian and American HSS manuals are very similar, this would be an incorrect conclusion to draw. The American HSS manual (AISC 1997a) is constructed to be very much consistent with the format and fundamental approach contained in all other AISC design manuals and as such takes a much more general approach to the promulgation of design guidelines. In contrast, the Canadian HSS manual (Packer 1997) is much more focused on the specific design case of the HSS truss. Most of the Canadian manual is focused to support the design of variations on the HSS truss form.

To discuss the state-of-art knowledge in steel HSS construction, it would be a mistake not to also consider work that is being done outside of North America. Both the Canadian and American HSS specifications have adopted significant material from the *Comite International pour le Developpement et l'Etude de la Construction Tubulaire* (CIDECT). Found in 1962, CIDECT is an international organization of major HSS manufacturers that was formed to combine all the resources worldwide from industry, universities, and other national and international bodies for research and application of technical data, development of simple design and calculation methods and dissemination of the results of research (Wardenier *et al.* 1991). CIDECT has technical and research activities ongoing in many areas of HSS construction including: buckling behavior of columns and trusses, bending strength of members, static strength of welded and bolted joints, and fatigue resistance of joints. Most germane to the current discussion on circular HSS connections is CIDECT's publication *Design Guide for Circular Hollow Section (CHS) Joints Under Predominantly Static Loading* (Wardenier *et al.* 1991). This publication contains capacity equations for many of the same HSS connections addressed in the Canadian and American specifications, but it also provides data for many other types of joints which will prove valuable for predicting the bearing capacity of circular HSS chord members; the focus of the present work.

### 3. Scope of experimental work

The experimental research program is aimed at quantifying the response of the bearing region in large-diameter HSS truss chords involving curved steel bearings and a Structural Tee intermediate member. The scope of the current experimental work is limited to concentric loading and is threefold: to determine the capacity of a particular truss bearing configuration through physical testing, to

evaluate the adaptability of existing provisions for predicting the bearing capacity of tubular truss chords in general; and to produce a data set of physical testing results for the purposes of validating nonlinear finite element modeling techniques to be used as part of future parametric studies.

#### 4. Description of test specimen and setup

The basis for the geometry of the specimens considered in the experimental tests reported on herein is the *Standard Drawings for Bridge Construction [and Design]* developed and maintained by the Pennsylvania Department of Transportation (PennDOT). The bearing configuration selected for consideration in this work can be found in many of the highway sign structure truss details contained in these standards. In an effort to maintain reasonable geometric parameters for testing, the experimental specimens are proportioned to exactly match the design and details emanating from BD-644M and BC-744M (PennDOT 2003a,b) for the case of a tri-chord truss spanning greater than 60 m (197'); which calls for three (3) - 12.7 mm  $\times$  660 mm (1/2"  $\times$  26") diameter HSS chords laced together with ST255  $\times$  71.5 (10  $\times$  48) members.

At the truss ends, the first ST intermediate member is oriented vertically and thus is normal to the sidewall of the HSS chord, and the chord end is seated in a curved saddle bearing assembly in close proximity to the ST. As a result of the ST orientation, and the fact that this location is highly stressed from the reaction forces, PennDOT chose to detail the ST to bear directly upon the HSS chord side wall through a full-penetration welded connection. In order to simulate this condition in the laboratory set-up, two curved saddles were proportioned and positioned within a specially built load frame whose proportions were consistent with those called out in BD-744M (PennDOT 2003b). In general, the schematic testing condition depicted in Fig. 3 was adhered to in the design of the specimens and load frame. Two (2) specimens having the same dimensions and loading conditions were tested in order that

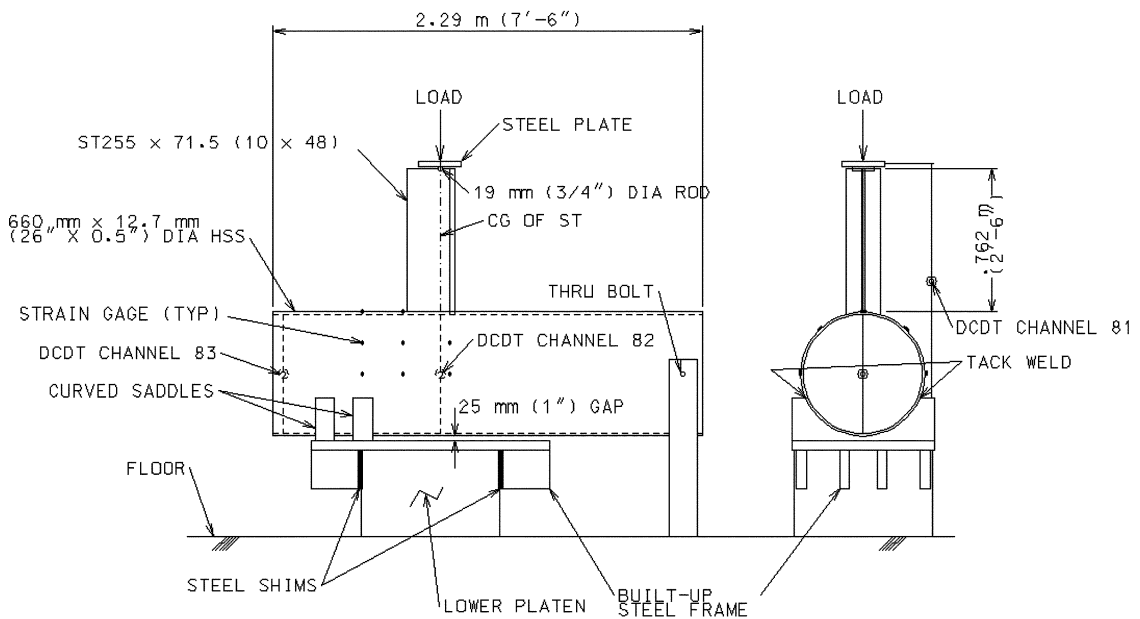


Fig. 3 Schematic of experimental test setup

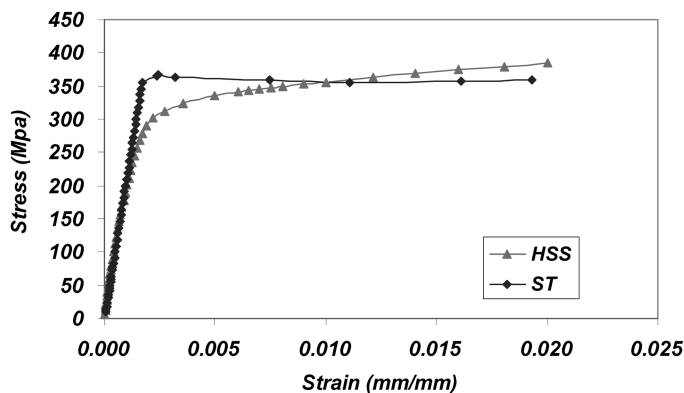


Fig. 4 Material response of steel used in specimens (representative coupon results)

repeatability of results within the testing program might be ascertained.

Fully nonlinear shell finite element based models of potential specimen geometries and the general testing configuration were first constructed and analyzed using ABAQUS (2003) as a means of identifying proportions that permitted economy in material and fabrication costs while at the same time preserving the integrity of the structural response and failure modes germane to the current work. In the end, the 660 mm (26") circular HSS component of the specimens was selected to be 2.29 m (7'-6") long and the ST255 × 71.5 (10 × 48) was specified to be 0.762 m (2'-6") long (as shown in Fig. 3). The HSS length was selected to provide a sufficiently long specimen such that continuity effects of adjacent HSS material would be preserved (i.e., the specimen had to be long enough to capture the local effects of continuity in HSS sidewall provided by the 60 m (197') + long piece as would be used in the field). The finite element models indicated that the 2.29 m (7'-6") length would be more than adequate for this purpose. Another consideration impacting the HSS length was related to the desire to have the end of the Circular HSS bear firmly against the saddles and not "lift-off" as a result of pivoting around the support of an excessively short HSS section. Finite element modeling indicated that the 2.29 m (7'-6") HSS length was sufficient to ensure realistic kinematics in the test. Similarly, the length of the ST255 × 71.5 (10 × 48) specified was arrived at through finite element modeling that indicated 0.762 m (2'-6") of member length would be sufficient to attenuate local effects from the point load applied to the top of the ST member by the loading frame actuator (i.e., 0.762 m (2'-6") was sufficient for ST. Venant's principle to take effect and disperse stress concentrations at the load point). In terms of boundary conditions on the circular HSS, at the end away from the saddle, a single thru-bolt was positioned close to the unloaded end of the HSS specimen in order to serve as a "pinned end." The grade of steel used for the HSS was ASTM A53 Grade B and the steel used for the ST255 × 71.5 (10 × 48) was ASTM A709 Grade 345 (50). The material stress-strain response curves obtained from coupon tests are shown in Fig. 4; the complete set of coupon testing results is reported elsewhere (Boyle 2004).

In order to compare the experimental test results to future finite element modeling results, the strains at certain critical points on the HSS section needed to be accurately measured. After reviewing the finite element models of the specimen geometries considered herein, it was decided that three rows of strain rosettes on the HSS section were required to capture the needed information. The first row fell directly over the saddle closest to the ST; the third was directly under the ST aligned with the center of the flange; the second row of rosettes was oriented at the midpoint between the two. Five rosettes were placed in each row, one at each 90 and 45 degree angular position around the cross-section, and one

located at the top of the HSS section as seen in Fig. 3. The third rosette row, located under the ST, did not have a rosette on top since the ST occupied the required location for installation. Three uniaxial strain gauges were also placed at the midpoint of the ST on each of the flange tips as well as on the web tip to measure the strains in the ST section.

In an effort to monitor deformations and cross-sectional distortion, three displacement transducers (DCDTs), identified as Channels 81, 82, and 83, were used to measure displacements at different locations. The locations were selected to reveal the portion of the overall specimen deformation that resulted from local wall distortion and the portion that resulted from global bending. The DCDT designated as Channel 81, was mounted externally to a bar that was attached to the lower platen of the loading frame, which served as a ground (fixed) point. This DCDT extended to the upper platen of the testing machine and thus it measured the total displacement including both global and local deformation effects within the specimen (i.e., both overall bending of the chord and ovalization of the chord cross-section). The DCDT designated as Channel 82, was positioned inside the HSS directly under the flange-web junction of the ST. This DCDT measured the relative displacement of the top and bottom walls of the HSS, which is the deflection due to local wall distortion under the ST. The final DCDT, Channel 83, was oriented in a similar fashion to Channel 82 inside the HSS, but in this case at the open end of the HSS directly over the saddles. The results of this DCDT will help to determine if any ovalization occurs at the open end, thus revealing to what extent the applied load is dispersed longitudinally.

As previously mentioned, the load was applied to the top of the ST using an actuator. The load was applied in 22 kN (5 kip) increments, which were held for approximately two minutes as the instrumentation was scanned and recorded using a computer controlled data acquisition system. In order to ensure minimal eccentricities at the point of load application, a semicircular notch was cut into



Fig. 5 Photograph of the experimental test specimen

the stem of the ST directly at the centroid of the cross section where load application occurred. A steel plate with a 19 mm (3/4") diameter rod (which fit directly into the notch) welded to the center was positioned into the notch and the load cell bore on the plate as the actuator applied the load. In this way, any incidental moment was released and not transmitted to the load cell.

## 5. Test results

The two (2) full-scale experimental tests were conducted in the Watkins-Hagaart Structural Engineering Laboratory at the University of Pittsburgh in August 2003 (see Fig. 5). The load versus deflection responses as recorded by DCDT channels 81, 82, and 83 for both experimental tests are shown in Figs. 6 and 7. The complete test data including the strain gage results is available in the report

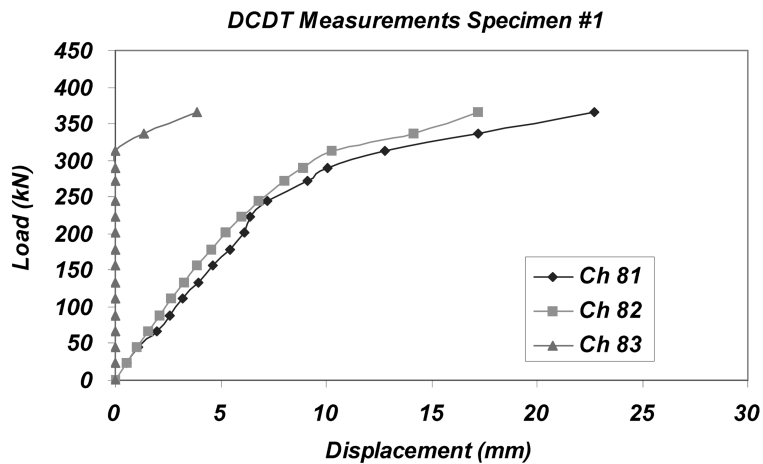


Fig. 6 DCDT measurements for Specimen #1

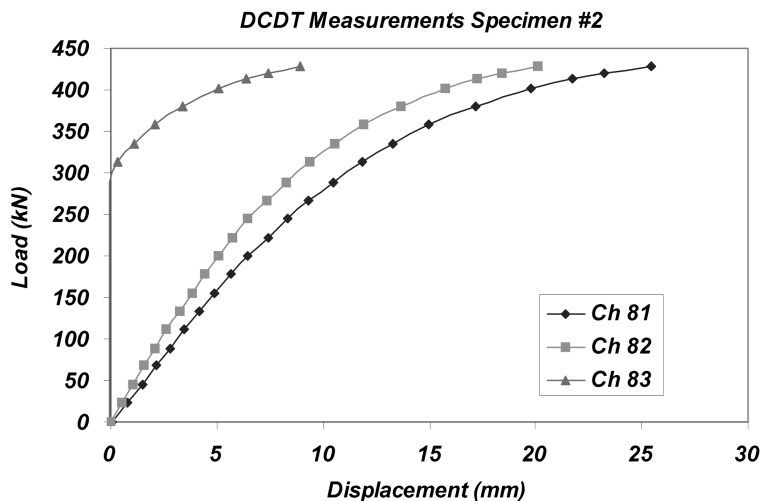


Fig. 7 DCDT measurements for Specimen #2

by Boyle and Earls (2004). Based on the deflection data alone, there are a number of important observations that can be made.

Both tests were completed without any significant problems. However, during the testing of Specimen #1, the thru-bolt at the opposite end yielded due to a bending overstress. Approximately midway through the test, the bolt began to sag, allowing the end to drop slightly. This allowed the HSS chord to rotate, and thus caused some undesired eccentricity (and moment) to be applied to the joint. The test was continued until failure, but it is believed that the ultimate load was reduced somewhat by the additional moment introduced into the ST as a result of the slight sagging associated with the thru-bolt. For Specimen #2, the thru-bolt size was increased and stiffening bars were added to decrease the span length for the bolt. As a result, the second test was completed without any plastic deformation of the thru-bolt. This is apparent by observing the smooth shape of the load-deflection plot for Specimen #2 as compared to Specimen #1.

Upon review of the DCDT measurements of both tests, it is observed that the majority of the displacement is due to local distortion or ovalization of the HSS cross-section. This is apparent by observing the small difference in the measured displacements of Channels 81 and 82 at any load. Recall that Channel 81 measured the total displacement at the ST including both global and local deformation effects within the specimen and Channel 82 measured the local deformation only. Since the difference between these two measurements remains relatively small for all loads, this indicates that there is little global deformation. This makes sense physically since the ST and saddles are in such close proximity and the internal moment arm generated between these two elements is quite small when considered from a practical standpoint.

The next observations made are relevant to the various limit states of failure for the bearing region. Three response features in the load-deflection history are identified that may be of importance in standard design practice. They are: 1) the yield load,  $P_y$  2) the ultimate load,  $P_u$  and 3) the nominal capacity load,  $P_n$ .

By analyzing the measurements of Channels 81 and 82, it appears that both specimens began to yield at a load of approximately 130 kN (30 kips). This is the load at which the non-linear behavior appears to have initiated, but a precise value is difficult to ascertain. Based on observations of the specimens during testing, it appeared that this yielding occurred in the HSS wall adjacent to each ST flange tip in the form of small "dimples." Depending on the structural application, this dimpling may not be considered objectionable. Since this yielding occurs at such a low load level and there is so much reserve capacity in the joint beyond this load, it is likely to be too costly to design the connection to prevent any yielding whatsoever.

The ultimate load of this connection is significantly higher than the yield load: Specimen #1 achieved an ultimate load of 365 kN (82 kips) and Specimen #2 achieved an ultimate load of 427 kN (96 kips). As mentioned previously, during testing of Specimen #1 a small moment was likely introduced in the specimen; it is suspected that this reduced the ultimate load for the test. Therefore, it is believed that the ultimate capacity should be considered as 427 kN (96 kips) rather than the average of the two tests until further testing is conducted. It should be noted that 427 kN (96 kips) is consistent with the ultimate load predicted by FEM analysis.

For defining the nominal capacity for the purposes of design, some judgment must be exercised. AISC has formulated many of its HSS provisions so that a deformation limit state is not exceeded at service loads (AISC 1997a). A similar approach is applied to the present results by analyzing the Channel 83 response, which is the DCDT located at the open end of the HSS. At the open end, the deflection remained at zero as the load increased through most of the test. But when the load reached

310 kN (70 kips), the deflection began to increase quickly and the ultimate load for the specimen was realized soon after that point. The previous result supports the notion that a collapse mechanism began to form at a load of 310 kN (70 kips) and the stability of the failure mechanism was in question once the open end began to close. It should also be noted that this behavior was observed to be repeatable across both tests. Thus, in the context of preventing excessive deformations, it is recommended that the point of initiation of the collapse mechanism should be considered as the nominal capacity. This is a slightly different approach than that utilized by AISC, but it is warranted due to the apparent unstable nature of the failure. Thus, the nominal capacity is considered as 310 kN (70 kips) based on the experimental testing.

## 6. Methods for predicting capacity

As mentioned previously, none of the referenced publications in the literature specifically address the bearing capacity in circular HSS truss chords. However, research has been done, and capacity equations developed, for many HSS connections that are related to this particular case of interest. An attempt has been made to identify existing provisions that are considered germane to the connection configuration studied herein, and that could be adapted for the purposes of estimating the bearing capacity.

The proposed methods are based on the assumption that the ST-to-chord joint is the “weak link” in the system and that overall capacity is governed by this detail alone. That is, the saddle bearings are assumed to adequately transfer the reaction force to the chord without compromising the overall capacity. However, the ST joint itself is not covered directly by existing specifications; and thus, existing provisions must be adapted further. Methods 1-3 are based on the limit state of chord wall plastification and Method 4 is based on the limit state of punching shear, both of which are potential mechanisms of failure that may govern the capacity the bearing region.

### 6.1. Method 1

In Section 8 of the LRFD HSS specification (AISC 2000), there are capacity equations provided for the case of a concentrated force applied to an unstiffened HSS wall through a single bearing plate. To

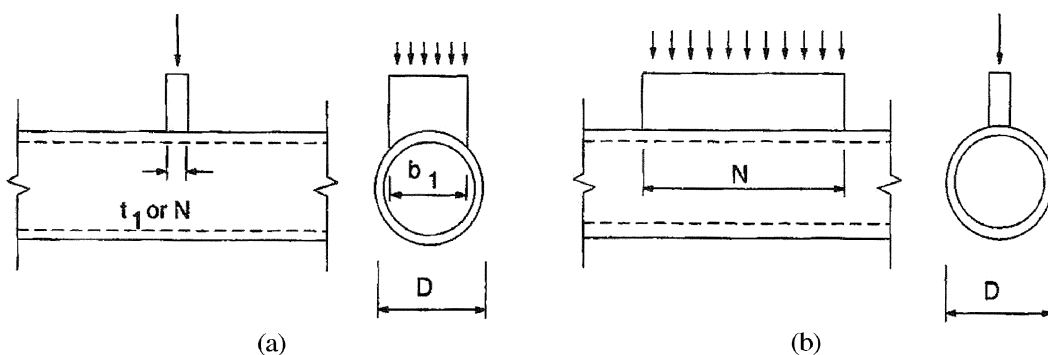


Fig. 8 (a) Concentrated force distributed transversely (AISC 2000), (b) Concentrated force distributed longitudinally (AISC 2000)

utilize these provisions, the ST member could be analyzed as two individual plates; one transverse and one longitudinal to the HSS axis. Section 8.1 addresses the case of a *Concentrated Force Distributed Transversely at the Center of the HSS Face*, and Section 8.2 addresses the case of a *Concentrated Force Distributed Longitudinally at the Center of the HSS Face* (see Fig. 8). These provisions may be applied by assuming that the ST connection will have a total capacity equal to the transverse plate capacity plus the longitudinal plate capacity, or direct superposition of the capacities. (Since this approach neglects any interaction between the two plates, this will prove to be unconservative which will be discussed later.)

Using this approach, the capacity of the transverse component (flange) is first calculated using the provision for a circular HSS subjected to a uniformly distributed transverse line load as shown in Section 8.1 (and reproduced below as Eq. 1):

$$R_n = \frac{5F_y t^2}{1 - 0.81 b_1 / D} Q_f \quad (1)$$

where,

$b_1$  ≡ the width of the load

$Q_f$  ≡ 1.0 for tension in the HSS (for compression see Eqn. 8.1-1 in AISC (2000))

$F_y$  ≡ specified minimum yield strength of the HSS

$t$  ≡ HSS wall thickness

$D$  ≡ HSS diameter

Similarly for the longitudinal component (stem), the capacity is based on the provision for a circular HSS subjected to a uniformly distributed longitudinal line load as shown in Section 8.2 (and reproduced here as Eq. 2):

$$R_n = 5F_y t^2 (1 + 0.25N/D) \cdot Q_f \quad (2)$$

where,

$N$  ≡ the bearing length of the load

$Q_f$  ≡ 1.0 for tension in the HSS (for compression see Eqn. 8.1-1 in AISC (2000))

$F_y$  ≡ specified minimum yield strength of the HSS

$t$  ≡ HSS wall thickness

$D$  ≡ HSS diameter

Both of these equations (including the subsequent equation for  $Q_f$ ) are identical to the “Factored Connection Resistance” equations presented in Table 11.2 of the Canadian HSS manual (Packer 1997) and the “Design Strength” equations shown in Fig. 25 (Types XP-1 and XP-2) of the CIDECT Design Guide (Wardenier *et al.* 1991). Unlike the American LRFD specification, the Canadian manual also provides additional insight for consideration of a cruxiform detail, which is an X-shaped open section with plates in both the longitudinal and transverse directions. It states that since the transverse plate connection is so much stronger than the longitudinal one, the cruxiform variation is not considered to be significantly stronger than the simple transverse connection (Packer 1997). Applying this same logic to the case of an ST would suggest that a reasonable conservative estimate of the capacity could be obtained by considering the transverse plate component only. However, it should be noted that this is based on the assumption the longitudinal component is smaller or of similar size to the transverse

component (Wardenier 1982). This notion will be further investigated in light of the experimental test results and calculations.

## 6.2. Method 2

A second type of joint that is similar to the ST connection for which published data is available is the HSS-to-HSS Truss Connection (see Fig. 9). This case is well researched and capacity equations are published in all of the previously mentioned references: American, Canadian, and CIDECT. Although at first glance it would seem that a ST and HSS are not very similar in geometry, the limit state that governs the capacity of both joints is chord wall plastification. And both the ST and HSS will actually generate similar yield line mechanisms at failure of the chord wall (see Fig. 10).

The provisions that apply to axially loaded circular HSS-to-HSS Truss connections are shown in Section 9.4 of the LRFD HSS specification (AISC 2000). Under subsection 2b, for branches with axial loads under the limit state of chord wall plastification, the capacity equation is given as:

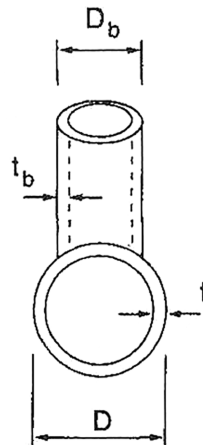


Fig. 9 HSS-to-HSS truss connection (AISC 2000)

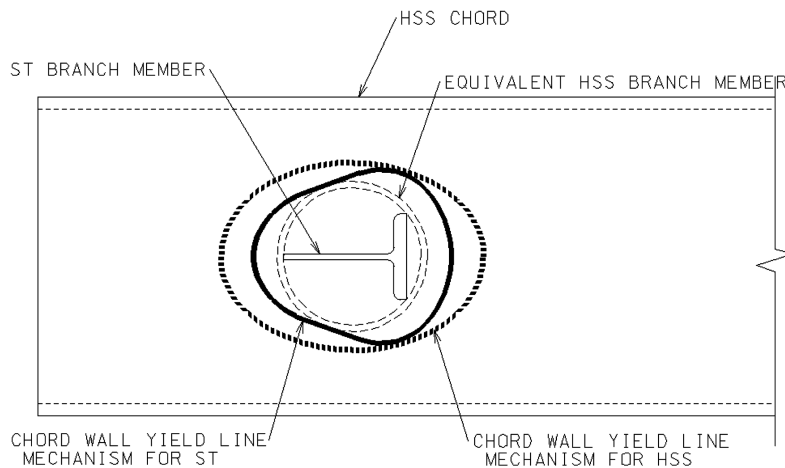


Fig. 10 Yield line mechanisms for ST and equivalent HSS branch members

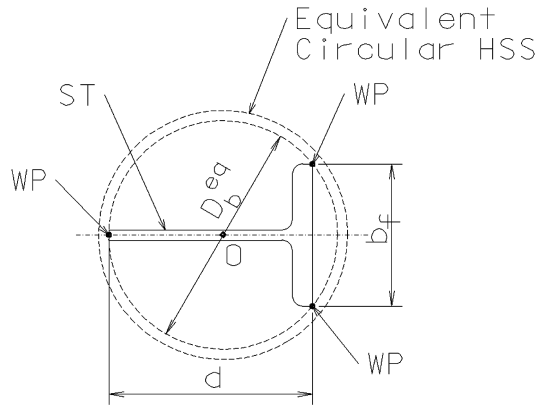


Fig. 11 Equivalent circular HSS diameter

$$P_n \sin \theta = t^2 F_y (6\pi \cdot \beta \cdot Q_q) \cdot Q_f \quad (3)$$

where,

$\theta \equiv$  Angle between the branch and chord

$\beta \equiv$  Branch Diameter / Chord Diameter

$Q_q \equiv$  see Eqn. (9.4-3) in (AISC 2000)

$Q_f \equiv$  see Eqn. (9.4-3) in (AISC 2000)

To apply this equation to the ST joint, an “equivalent” branch diameter must be calculated for the ST member. This is the branch diameter that will generate a yield line mechanism similar to the one that will form in the ST joint at failure. A reasonable approach for this is to use the diameter that exactly circumscribes the ST footprint. That is, the diameter of a circle that intersects the tips of each flange and stem (see Fig. 11). To calculate the equivalent diameter in this way for an arbitrary ST shape, the following formula can be used:

$$D_{b,eq} = b_f^2 / 4d + d \quad [\text{for } b_f < 2d] \quad (4)$$

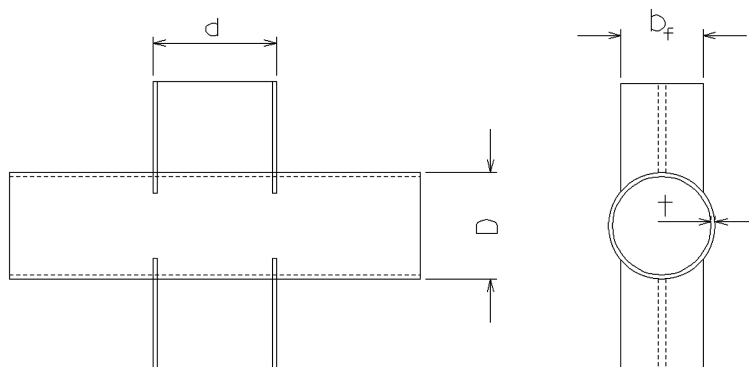


Fig. 12 WT-to-HSS joint covered by CIDECT

### 6.3. Method 3

A third HSS joint that is similar to the ST connection for which published data is available is the case of a wide flange I-shape end-connected to a circular HSS (see Fig. 12). This case is covered only in the CIDECT Design Guide (Type XP-4), where a capacity equation is provided. The capacity equation for this case combines Eqs. (1) and (2) to yield the following (recast in LRFD format):

$$R_n = \frac{5F_y t^2}{1 - 0.81 b_f / D} \cdot (1 + 0.25 \cdot d / D) \cdot Q_f \quad (5)$$

Intuitively, a joint with a W shape branch member should yield a higher capacity than a ST member of the same depth due to the simple fact that there are two flanges, not one (oriented transversely to the HSS axis). And as stated previously, the Canadian manual suggests that transverse plate components have the greatest effect on the overall strength of the connection. However, the case of a W shape connected to a circular HSS may actually behave like the ST connection more than the case of a concentrated load applied through a single transverse plate; as will be seen subsequently. As noted for the HSS-to-HSS joint, the geometry of the chord wall yield lines at failure for both the W and ST joints should be similar.

### 6.4. Method 4

The last important consideration relevant to the ST joint is the limit state of punching shear in the chord wall. Research has shown that this mode of failure can be important in plate-type connections and it may prove to govern the capacity depending on the geometry of the joint. This limit state is addressed in all of the previously mentioned references (with subtle differences in load factors and philosophy): American, Canadian, and CIDECT. The American LRFD specification is somewhat different in that the provision is framed to prevent shear *rupture*, while the Canadian and CIDECT provisions take the approach of preventing shear *yielding*. Since neither specimen exhibited a failure by rupture, the latter approach is more applicable. In the Canadian specification (Packer 1997), the punching shear capacity is checked using Eq. (9.19) (reproduced below as Eq. 6 recast in American LRFD format, neglecting bending):

$$\frac{R_n}{A} \cdot t_p = 1.16 F_y \cdot t \quad (6)$$

This equation can be rewritten for calculating the nominal branch axial load capacity for the limit state of punching shear as follows:

$$R_n = 1.16 F_y A \cdot t / t_p \quad (7)$$

In applying this equation to the ST joint, it is recommended that the flange area alone be used for the value of A. The transverse plate component will transfer most of the load to the chord during a punching shear failure due to the relative flexibility of the HSS wall between the transverse and longitudinal directions.

### 6.5. Additional notes

It should be noted that there are a number of limits of applicability listed in Section 9.4 (2a) of the LRFD HSS specification (AISC 2000) that should be considered. Most relevant to the ST joint are the limits on wall stiffness (3) and the limit on width ratio (4). The limit on wall stiffness states that the ratio of diameter to wall thickness must be less than or equal to 50 for chords and branches in T-, Y-, and K-connections and less than or equal to 40 for chords of Cross-connections. Members that exceed this limit would be classified as thin-walled sections. The limit on width ratio states that the ratio of branch diameter to chord diameter be within the range:  $0.2 < D_b/D < 1.0$ .

These limits are specified since some of the published limit state expressions (or their calibrations) are partly empirical. Although the design recommendations have been developed based on many experimental tests and research that has been carried out worldwide, the formulas may not be reliable outside the parametric range for which they have been validated (AISC 1997a). Thus, it is prudent to use a set of parameter limits that reflect the bounds of most test results.

It should also be noted that for all capacity calculations described above, a design wall thickness “ $t$ ” is needed. When the actual wall thickness is not known, a value of 0.93 times the nominal thickness is permitted to be used as recommended by AISC (2000). This recommendation arises out of the fact that the American Society of Testing Materials (ASTM) permits the wall thickness in HSS fabrication to be as much as 10% below the nominal thickness.

## 7. Validity of proposed methods

To assess the validity of the proposed methods, the various capacity equations have been applied to the geometry of the experimental test and these predictions are then compared to the results obtained from the experimental testing program reported on herein. The relevant detail geometry that is considered in the application of the capacity equations is the diameter, thickness, and material strength of the HSS chord and the section dimensions for the ST255×71.5 (10×48). This data is summarized below:

### ST255×71.5 (10×48)

$$b_f = 183 \text{ mm (7.2")}$$

$$t_f = 23.4 \text{ mm (0.92")}$$

$$d = 258 \text{ mm (10.15")}$$

$$t_w = 20.3 \text{ mm (0.8")}$$

### HSS Chord

$$D = 660 \text{ mm (26")}$$

$$t = 12.7 \text{ mm (0.50")}$$

$$F_y = 331 \text{ MPa (48 ksi)*}$$

\*based on coupon test results

To apply the proposed equations to the experimental test, some assumptions will have to be made. The first assumption is with respect to the  $Q_f$  factor, which is relevant to proposed Methods 1-3. Since the ST is slightly offset in the longitudinal direction from the saddle support below, some flexural stress will develop in the HSS causing tension in the bottom face and compression in the top face. Compression in the chord wall at the ST will likely cause some reduction in the joint capacity. However, due to the close proximity of the ST and saddle, most of the load will likely be transferred by direct shear, or so-called “deep beam” action. Thus, it seems reasonable to neglect any capacity reduction resulting from bending stress and assume  $Q_f = 1.0$ .

The second assumption to be made is whether this connection should be classified as a T-connection or a Cross-Connection, which is relevant to Method 2. The AISC HSS specification states that when the branch load is equilibrated by beam shear in the chord member, the connection shall be classified as a T-Connection, but when the branch load is transmitted through the chord member and is equilibrated by branch members on the opposite side, the connection shall be classified as a Cross-Connection (AISC 2000). Unfortunately, the tested configuration falls somewhere in between these two ideals, as mentioned before. Due to the close proximity of the ST and saddle bearing below, it seems reasonable to assume that most of the load is transferred directly through the HSS by shearing action with little bending stress developing. Thus, the connection might be seen to behave more like a cross-type connection.

Before applying the proposed methods, the limits of applicability mentioned in the previous section should also be considered in light of the test specimen geometry. First, the limit on wall stiffness ratio is 40 for cross connections as specified in the LRFD HSS Specification (AISC 2000). This ratio for the test specimens is  $660/12.7 = 52$ , which is, in fact, slightly outside of the specified limit. Second, the width ratio should fall within the specified limits of 0.2 to 1.0 (AISC 2000). Utilizing the ST flange width ( $b_f$ ) as the branch diameter yields a width ratio of  $183/660 = 0.28$ , which is within the specified limit. Although the wall stiffness ratio has been exceeded, this does not disqualify the use of the provisions as proposed. The limits are merely being considered to evaluate how the specimen geometry compares to joint configurations studied previously.

Utilizing these assumptions and the known geometry, the capacity of the ST joint in the experimental test has been calculated using the proposed methods developed earlier:

- **Method 1:** Applying the provision for a concentrated force distributed transversely at the center of the HSS Face (Eq. 1) yields:

$$R_n = \frac{5(331\text{MPa})(12.7\text{mm} \cdot 0.93)^2}{1 - 0.81(183\text{mm})/(660\text{mm})}(1.0) = 297\text{kN}(67\text{kips})$$

Applying the provision for a concentrated force distributed longitudinally at the center of the HSS Face (Eq. 2) yields:

$$R_n = 5(331\text{MPa})(12.7\text{mm} \cdot 0.93)^2(1 + 0.25(258\text{mm})/(660\text{mm})) \cdot (1.0) = 253\text{kN}(57\text{kips})$$

- **Method 2:** To apply the provision for a HSS-to-HSS truss connection, the equivalent branch diameter and the  $Q_q$  factor must first be calculated using Eq. (4) and LRFD Eq. (9.4-3):

$$D_{b,eq} = (183\text{mm})^2/4(258\text{mm}) + (258\text{mm}) = 290\text{mm}(11.4")$$

$$Q_q = \left( \frac{1.7}{2.4} + \frac{0.18}{(290\text{mm}/660\text{mm})} \right) \cdot (1.0)^{0.7(2.4-1)} = 1.12$$

The capacity is then calculated using Eq. (3) as follows:

$$P_n(1.0) = (12.7\text{mm} \cdot 0.93)^2(331\text{MPa})(6\pi \cdot (290\text{mm}/660\text{mm}) \cdot (1.12)) \cdot (1.0) = 428\text{kN}(96\text{kips})$$

Table 1. Comparison of results

Experimental		Theoretical			
Nominal	Ultimate	Method 1	Method 2	Method 3	Method 4
310 kN	427 kN	297 kN/253 kN	428 kN	326 kN	829 kN

- Method 3: Applying the provision for a W-to-HSS joint (Eq. 5) yields:

$$R_n = \frac{5(331\text{MPa})(12.7\text{mm} \cdot 0.93)^2}{1 - 0.81(183\text{mm})/(660\text{mm})} \cdot (1 + 0.25 \cdot (258\text{mm})/(660\text{mm})) \cdot (1.0) = 326\text{kN}(73\text{kips})$$

- Method 4: Applying the punching shear provision (Eq. 7) yields:

$$R_n = 1.16(331\text{MPa})(183\text{mm} \cdot 23.4\text{mm}) \cdot (12.7\text{mm} \cdot 0.93)/(23.4\text{mm}) = 829\text{kN}(186\text{kips})$$

The theoretical results from each proposed method along with the experimental results are summarized in Table 1.

## 8. Discussion

In light of the experimental and theoretical results, it must be said that there may be a fundamental problem with using the proposed methods for predicting the capacity of the bearing in this geometric configuration. The vicinity of the connection to the open end of the HSS chord has influenced the geometry of the yield line failure mechanism observed experimentally and so too then, the overall capacity based on observations of the test data. However, all of the existing specifications that were used in the development of the proposed methods were based on research done on a typical interior joint with a continuous chord member (i.e., not near an end). Without further investigation, it is unknown to what level the open end has affected the capacity of the joint. However, it is also pointed out that ovalization of the open end did not develop until load level of greater than 75% of ultimate capacity were achieved; an observation somewhat at odds with the notion of significant restraint effects being present due to adjacent sections. In any case, it can be surmised that the open end can only serve to *reduce* the capacity from that of an interior connection detail vis-à-vis the capacity at an interior location.

For the bearing detail under consideration, the flange of the ST member was located a distance 842 mm (33") from the end of the HSS, or a distance of  $5/4 \times D$ . If the proposed methods are shown to be accurate for this geometry, they will *underestimate* the capacity of another joint with an end distance greater than this. Similarly, the proposed methods will *overestimate* the capacity of joints located in closer proximity with the open end. Future finite element studies, using validated modeling strategies, will be used to explore this point further as part of ongoing research.

### 8.1. Method 1

The theoretical capacity predicted by Method 1 is 297 kN (67 kips) for the transverse component (flange plate) and 253 kN (57 kips) for the longitudinal component (stem plate). As mentioned above, the recommendation given the Canadian HSS manual is that only the transverse component should be

considered in this case. Applying this notion to the ST joint yields a net theoretical capacity of 297 kN (67 kips), which agrees very well with the nominal capacity of 310 kN (70 kips) indicated by the experimental results, being within 5%. Adding the capacities of the individual components by direct superposition would result in a net theoretical capacity of 550 kN (124 kips), which is a significant overestimate of the nominal capacity, and therefore considered inaccurate in this case.

Although superposition of the individual plate component capacities is unconservative for calculating the nominal capacity, it may apply to the calculation of the ultimate capacity. This recognizes that there is some increase in the ultimate connection capacity attributable to the presence of the longitudinal plate component. However, direct superposition once again overestimates the ultimate capacity of 427 kN (96 kips) obtained from the experimental results by a significant margin (30%). Assuming that the transverse plate component dominates the overall capacity as before, then it may be reasonable in this case to add the transverse component capacity plus a fraction of the longitudinal component capacity. Using a somewhat arbitrary 50% factor on the longitudinal plate component yields a theoretical capacity of  $297 + (0.50 \times 253) = 424$  kN (95 kips), which compares well with the experimental results. However, Method 2 is preferred for calculating ultimate capacity as discussed below.

### *8.2. Method 2*

The theoretical capacity predicted by Method 2 is 428 kN (96 kips), which is an overestimate of the nominal capacity from the experimental data by a margin of 38%. This lack of correlation to the nominal capacity is likely attributable to the influence of the open end of the HSS on the governing failure mechanism as discussed previously. Because this appears to be significant in this case, Method 2 is not recommended for the calculation of the nominal capacity of the joint under consideration.

Although the agreement with the nominal capacity is inadequate, this method predicts the ultimate capacity very well (to within 0.2%). However, it is not fully understood why this is so. Since the ultimate joint capacity is governed by the limit state of chord wall plastification, then the capacity is proportional to the total length of the yield lines in the failure mechanism. It is possible that the mechanism at work in the current geometric configuration happens to have the same total length of yield lines in the chord wall as the mechanism for an interior joint; the basis of the proposed method. Although this question remains, Method 2 is recommended for calculation of ultimate capacity due to the good agreement to the experimental results.

It should be mentioned that there is significant motivation for using Method 2 since it is the most portable of all the proposed methods. That is, it can be applied to many different connection geometries such as T-, Y-, K-, and Cross-connections, and it also treats the case wherein the branch member(s) experience flexure in addition to axial load. However, since the current research has only considered the axially loaded 90° cross-connection, extending this method to other connection types should be done with care.

### *8.3. Method 3*

The capacity predicted by Method 3 is 326 kN (73 kips), which agrees with the nominal capacity from the experimental results to within 5%. As described earlier, this method is based on the CIDECT provision for a wide-flange connection, which is similar to the ST joint being studied except for the additional flange. This seems to imply that the additional flange does not significantly increase the overall strength of the joint.

#### 8.4. Method 4

The capacity predicted by Method 4 is 829 kN (186 kips), which does not agree well with the experimental results. Recalling that this method is based on the limit state of punching shear indicates that the capacity of the ST joint in this case is not governed by punching shear. However, this limit state is still considered relevant to the connection since it may control for certain geometries. In particular, punching shear will likely govern the capacity of the ST joint when the flange width ( $b_f$ ) is small in comparison to the HSS chord diameter.

### 9. Conclusions

Two (2) full-scale experimental tests were performed on a long-span tubular truss bearing region consisting of a 12.7 mm  $\times$  660 mm (1/2"  $\times$  26") diameter HSS chord seated in curved steel bearings with a ST255  $\times$  71.5 (10  $\times$  48) intermediate member connected at 90° at a distance of 842 mm (33") from the open end of the chord. The experimental results indicate that the yield load is approximately 130 kN (30 kips), the nominal capacity is 310 kN (70 kips), and the ultimate capacity is 427 kN (96 kips). There is evidence that the vicinity of the connection to the open end of the HSS chord has reduced its overall capacity, but to what extent is unknown at this time. Ongoing research will address this question.

Four (4) methods are proposed for predicting the bearing capacity in simple-span tubular trusses based on modified application of existing US and international specifications. Method 1 and Method 3 are observed to provide accurate predictions for the nominal bearing capacity; both being within 5% of the experimental results. Method 2 produces an accurate prediction of the ultimate capacity, to within 0.2%. Method 4 is based on a limit state that did not control the failure of the test specimen; therefore, its accuracy could not be determined.

### References

- ABAQUS (2003), *ABAQUS Theory Manual*, Hibbitt, Karlsson & Sorensen, Inc., Pawtucket, Rhode Island, USA.
- AASHTO (2001), Standard Specifications for Structural Supports for Highway Signs, Luminaires and Traffic Signals, 4<sup>th</sup> Edition, *American Association of State Highway and Transportation Officials, Inc.*, Washington D.C.
- AISC (2000), "Load and resistance factor design specification for steel hollow structural sections", *American Institute of Steel Construction*, Chicago, Illinois, November 10.
- AISC (2001), "Manual of steel construction - load and resistance factor design 3<sup>rd</sup> edition", *American Institute of Steel Construction*, Chicago, Illinois, November.
- AISC (1997a), "Hollow structural sections connections manual", *American Institute of Steel Construction*, Chicago, Illinois.
- AISC (1997b), "Specification for the design of steel hollow structural sections", *American Institute of Steel Construction*, Chicago, Illinois, April 15.
- AWS (2004), D1.1 Structural Welding Code - Steel 19<sup>th</sup> Edition, *American Welding Society*, Miami, Florida, October 15.
- Boyle, R. and Earls, C. J., (2004), "Full-scale testing of tri-chord sign structure connections", Report No. CE/ST 28, Department of Civil and Environmental Engineering, University of Pittsburgh, Pittsburgh, Pennsylvania.
- Boyle, R. (2004), "Experimental testing of hollow circular section bearing capacity", M.S. Thesis, Department of

- Civil and Environmental Engineering, University of Pittsburgh, Pittsburgh, Pennsylvania. <http://etd.library.pitt.edu/ETD/available/etd-07152004-103115/>.
- Li, Y. and Earls, C. J. (2002), "Design recommendations for the proportioning and detailing of long-span tri-chord sign structures, Phase I", Report No. CE/ST 24, Department of Civil and Environmental Engineering, University of Pittsburgh, Pittsburgh, Pennsylvania.
- Packer, J. A. and Henderson, J. E. (1997), "Hollow structural section connections and trusses", second edition, *Design Guide*, Canadian Institute of Steel Construction, Willowdale, Ontario, Canada, June.
- PENNDOT (2003a), "Overhead sign structures - 2-Post & 4-Post Tri-chord truss spans from 18 288 to 73 152 (60' to 240') notes and design criteria", *Standard Drawings for Bridge Design - BD 644-M*, Commonwealth of Pennsylvania Department of Transportation, Harrisburg, Pennsylvania.
- PENNDOT (2003b), "Overhead sign structures - 2-Post & 4-Post tri-chord truss spans from 18 288 to 73 152 (60' to 240') notes and design criteria", *Standard Drawings for Bridge Construction - BC 744-M*, Commonwealth of Pennsylvania Department of Transportation, Harrisburg, Pennsylvania.
- Wardenier, J., Kurobane, Y., Packer, J. A., Dutta, D. and Yeomans, N. (1991), "Design guide for circular hollow section (CHS) joints under predominantly static loading", CIDECT (ed.) and Verlag TUV Rheinland GmbH, Koln, Federal Republic of Germany.

CC